Original Paper

Spectroscopic investigation of tissue-specific biomass profiling for *Jatropha curcas* L.

Taiji Watanabe[1], Amiu Shino[2], Kinya Akashi[3], Jun Kikuchi[1,2,4,5,*]

[1] Graduate School of Nanobiosciences, Yokohama City University, Yokohama, Kanagawa 230-0045, Japan; [2] RIKEN Plant Science Center, Yokohama, Kanagawa 230-0045, Japan; [3] Graduate School of Biological Sciences, Nara Institute of Science and Technology, Ikoma, Nara 630-0192, Japan; [4] Biomass Engineering Program, RIKEN Research Cluster for Innovation, Wako, Saitama 351-0198, Japan; [5] Graduate School of Bioagricultural Sciences and School of Agricultural Sciences, Nagoya University, Nagoya, Aichi 464-8601, Japan
* E-mail: kikuchi@psc.riken.jp   Tel: +81-45-503-9490   Fax: +81-45-503-9489

Abstract   The current focus of *Jatropha curcas* L. (Euphorbiaceae) research concerns the biodiesel obtained from the seed. However, the plant is an interesting source of biomass, and it has been applied in various ways. The characterization of the different parts of the plant is very important for better use of the residual biomass after oil harvesting. We divided Jatropha samples into seven samples: leaf, stem, bark, xylem, pith, seed coat and kernel, and their characterization was made using two spectroscopic techniques, namely Fourier transform infrared (FTIR) and nuclear magnetic resonance (NMR). Xylem and seed coat accumulate lignin and possibly *O*-acetyl-4-*O*-methylglucurono-β-D-xylan hemicellulose. Xylem lignin was richer in syringyl units and seed coat lignin was richer in guaiacyl units. Leaf, pith and bark accumulate cellulose and no *O*-acetyl-4-*O*-methylglucurono-β-D-xylan hemicellulose, and the kernel had a low rate of lignocellulose.

Key words: Biomass, *Jatropha curcas* L., nuclear magnetic resonance (NMR).

The current focus of *Jatropha curcas* L. (Euphorbiaceae) is mainly the production of oil from the seeds, but the biomass from the plant offers many other potentially useful products. The residue of the seed can be used for animal feed and biochar, the fibers can be used for construction and fertilizers, and the seed shell, rich in lignin, may be used for energy generation (Kurmar and Shama 2008; Manurung et al. 2009; Openshaw 2000).

Biomass mainly originates from the plant cell wall and comprises predominantly polysaccharides (cellulose, hemicellulose) and lignin, containing lignocellulose. Cellulose is a β-1,4-linked glucose molecule and all hemicellulosic polysaccharides contain a β-linked sugar backbone. In xylans, mannans, and xyloglucans, the backbone sugars are β-1,4-D-xylose, β-1,4-D-mannose, and β-1,4-D-glucose, respectively, while in glucomannan, the backbone consists of randomly dispersed β-1,4-glucose and β-1,4-mannose sugars. The backbones of hemicellulosic polysaccharides are decorated with a variety of sugars and acetyl groups (Gilbert 2010). Lignins are complex racemic aromatic heteropolymers, derived from three monomers (monolignols), *p*-coumaryl, coniferyl and sinapyl alcohols. These monolignols produce, respectively, *p*-hydroxyphenyl (H) guaiacyl (G) and syringyl (S) units when incorporated into the lignin polymer. Guaiacyl and syringyl can be found in the α-ketone structure (G′, S′). The coupling of the lignin units leads to the following substrutures: β-*O*-4 (A), β-5 (B), β-β (C), 5-5/4-*O*-β (D), 5-*O*-4 (E) and β-1 (F) (Boerjan et al. 2003; Kim and Ralph 2010).

For analysis of lignocellulose, nuclear magnetic resonance (NMR) techniques are widely used (Kikuchi et al. 2011). Yelle et al. 2008, and Kim and Ralph 2009 characterized the cell wall of gymnosperm; *Pinus taeda* (Loblolly pine), angiosperms; *Populus tremuloides* (Quaking Aspen), *Hibiscuus cannabinus* (Kenaf) and *Zea mays* (Korn) using a two-dimensional (2D)-NMR heteronuclear single quantum coherence (HSQC) technique, but this kind of analysis has never been conducted with *Jatropha curcas*. The use of this technique allows direct detection of substructures such as A, B, C, and D, besides the lignin units and polysaccharides, and can provide a more specific analysis of lignocellulose. However the assignment of the cross peaks from NMR
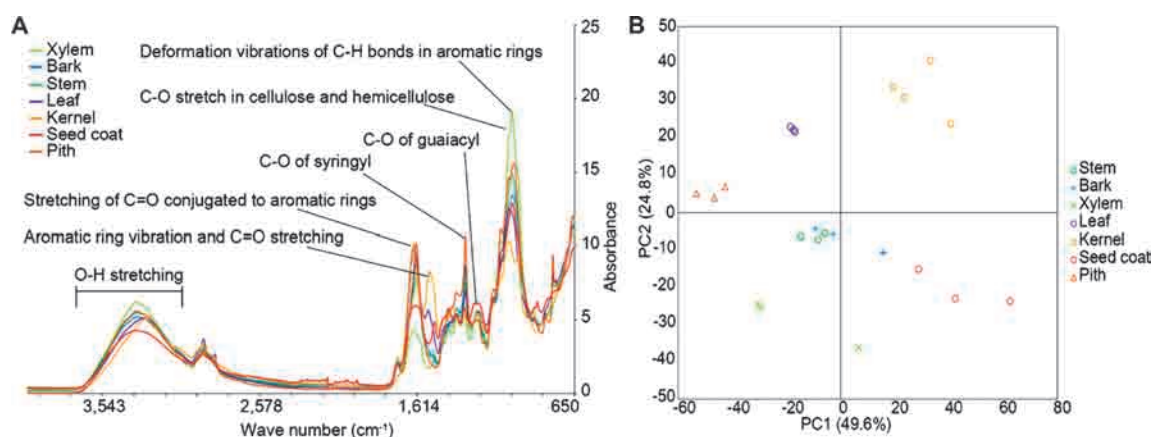
Figure 1. FTIR results from xylem, bark, stem, leaf, kernel, seed coat and pith. FTIR features assigned on O–H stretching (~3600 cm^{-1}–~3000 cm^{-1}), aromatic vibration and C=O stretching (~1622 cm^{-1}), stretching of C=O conjugated to aromatic rings (~1529 cm^{-1}), C–O of syringyl units (~1315 cm^{-1}), C–O of guaiacyl units (~1267 cm^{-1}), C–O stretch in cellulose and hemicellulose (~1028 cm^{-1}) and deformation vibrations of C–H bonds in aromatic rings (~1032 cm^{-1}) (a) PCA score plot of triplicate measurements of these seven tissues (b).

analysis is still not complete (Balakshin et al 2010).

Pretreatments of biomass products are essential in some situations when they are employed in energy generation or in biochar manufacture. One of the techniques employed is known as torrefaction and is a thermal pretreatment where the biomass is heated in the range 200–300°C (Chen and Kuo 2011). Knowledge of the composition of the biomass is important in order to carry out pretreatment in an effective manner.

The objective of the current research was to characterize the different tissues and organs of *Jatropha curcas* for future research concerning biomass applications.

Materials and methods

Samples from stem, seed and leaf were collected. The stem was analyzed as a single sample and divided in three parts: pith, xylem and bark, with the last sample including bark itself and phloem. The seed was divided into the kernel; comprising endosperm and embryo, and the seed coat. The samples were dried and ground, then low molecular weight components were extracted using distilled water and 100% methanol. The seed samples were also treated with hexane in order to extract the oil. These samples were used for attenuated total reflectance FTIR (Fourier transform infrared) spectroscopy using a Nicolet 6700 spectrometer and triplicate measurements.

For the analysis of NMR, samples were ball milled for 12 h with intervals of 10 min of pause between 10 min of grinding. Then the samples were dissolved in dimethylsulfoxide (DMSO)-d_6/pyridine-d_5 (4:1) in the proportion of 80 mg of sample in 800 μl (20 mg in 600 μl in the case of pith) and transferred to the NMR tube. These NMR samples were measured using 2D HSQC, 2D HSQC-total correlation spectroscopy (TOCSY) and 2D HSQC-nuclear Overhauser effect correlation spectroscopy (NOESY). All NMR measurements were obtained using a Bruker DRX-700

spectrometer calibrated at 318K, with 32 scans for 2D HSQC and 64 scans for 2D HSQC-TOCSY and 2D HSQC-NOESY. The central DMSO solvent cross peak was used as the internal reference (δ_C 39.5, δ_H 2.49 ppm).

For the relative quantification of lignocellulose we used the cross peak intensity from the carbon 1 of polysaccharides. Lignin units and substructures which we used were: A-H/Gα, A-Sβ, Aα, Bα, Cα, G5/6, G′5/6, H2/6, S2/6, S′2/6, Xlγ. Cross peaks with overlap of two carbons were divided by 2. The sum of the cross peak intensity of assigned lignin structures and polysaccharides were taken as 100%. To estimate the S/G ratio, we used the intensity of the cross peaks from G5/6, S2/6 and H2/6 and considered their sum as 100% (Ibirra et al. 2007; Ralph et al. 2006). PCA (principal component analysis) was performed using free software R, essentially similar to that used in our previous reports (Tian et al. 2007; Fukuda et al. 2009; Okamoto et al. 2009; Nakanishi et al. 2011).

Results

Overall characterization by FTIR

The FTIR peaks were assigned according to Pandey 1999 and Ke et al. 2011. The first peak in FIIR analysis to be considered for Figure xylem, bark, stem and seed coat samples is (Figure 1a), centered at ca. 3,332 cm^{-1} with no shoulder and, moreover, xylem was associated with the highest intensity. Leaf and kernel showed a broader peak centered at ca. 3,280 cm^{-1} and a shoulder at ca. 3,068 cm^{-1}, indicating a more complex hydrogen-bonding system, similar to that found for gymnosperm (Kubo and Kadla 2005). Kernel showed the highest intensity peaks related to aromatics rings at approximately 1529 cm^{-1} and 1622 cm^{-1}. Seed coat has the highest intensity peak in the guaiacyl C–O region (ca. 1267 cm^{-1}). Xylem showed the highest intensity peak of cellulose and hemicellulose stretch (ca. 1028 cm^{-1}) and a peak due to the deformation vibrations of C-H bonds

in aromatic rings (ca. 1030 cm^{-1}). Bark, pith, leaf and stem presented high intensity peaks in the C–O syringyl region (ca. 1315 cm^{-1}).

It is notable that the pattern of the chemical composition in each tissue is different, as is clear from PCA analysis (Figure 1b). For more specific data, we used the NMR techniques, and assigned the peaks according to past reports and applied 2D HSQC-TOCSY and NOESY to confirm the assignments as far as possible.

Annotation of lignocellulose components in 2D HSQC spectra

We assigned the cross peaks of polysaccharides in the anomeric region as much as possible according to past reports, but there remained a numbers of peaks to be identified (Kim and Ralph 2009; Ralph 2006). We have reported assignments for small biomolecular mixtures using NMR (Kikuchi et al. 2004; Kikuchi and Hirayama 2007; Chikayama et al. 2008; Mochida et al. 2009; Chikayama et al. 2010; Sekiyama et al. 2010), and essentially the same method was employed for biomacromolecular mixtures such as lignocellulose components (Ogata et al. 2012). In this analysis, it is possible to note differences in the patterns of the spectra of each tissue (Figures 2, 3). Comparing the spectra from the anomeric region from each sample (Figure 3), β1,4-D-glucopyranoside [(1-4)-β-Glc$p$/δ_C 101.5, δ_H 4.39] is present in all the tissues. Kernel showed the lowest number of spectral features and pith displayed the highest. Seed coat lacks α-L-fucopyranoside (α-L-Fuc$p$/δ_C 100.67, δ_H 5.16 ppm) and one of the α-L-arabinofuranoside (α-L-Ara$f$/δ_C 107.25, δ_H 5.07 ppm) cross peaks, which is found in all other samples. Bark and leaf spectra share some similar patterns, in that both lack α-D xylopyranoside (α-D-Xyl$p$/δ_C 92.03, δ_H 5.00). The spectrum for kernel has a unique pattern of polysaccharides. Acetylated xylopyranosides (3-O-Ac-β-D-Xyl$p$/δ_C 101.40, δ_H 4.48, 2-O-Ac-β-D-Xyl$p$/δ_C 62.95, δ_H 3.35) are not found, nor is α-D-Xyl$p$. Xylem and pith have all the identified cross peaks, though it is clear from the differences in the complexity of the signals that the pith showed more intense cross peaks and a more complex pattern of signals.

From the analysis of the aromatic region of the 2D-HSQC (Figure 2), the seed coat has the largest amount of lignin followed by xylem. Kernel and pith have some cross peaks that might be lignin signals, but they present the characteristic pattern of amino acids. The cross peaks enclosed by a square are those that overlap the lignin signals. It is seen that kernel and pith were considered to have low lignin content. Bark and leaf also present a similar pattern of amino acid signals, but it possible to verify that some signals arise from guaiacyl (G) and syringyl (S) units in bark and G units in the leaf sample.

Confirmation of assignments using 2D HSQC-TOCSY and HSQC-NOESY

The confirmation of the assignments was made through the correlation signals in the 2D HSQC-TOCSY and 2D HSQC-NOESY results. In Figure 4 the full lines represent the correlation present in TOCSY and NOESY analyses and the dotted lines represent those present only in NOESY.

This approach in the analysis is important due to the fact that the temperature used for the NMR work in this research is 318 K, and this may influence the chemical shifts of some cross peaks and move them from published values. Therefore the confirmation of the assignments was carried out as far as possible.

Through the correlation signals from 2D HSQC-TOCSY and 2D HSQC-NOESY spectra (Figure 4), it was possible to identify 2-acetyl-xylopyranoside (2-O-Ac-Xyl$p$) carbon 1 (C1) and carbon 2 (C2), in the chemical shift of δ_C 99.35, δ_H 4.58 ppm and δ_C 73.15, δ_H 4.65 ppm respectively. Other cross peaks of 2-O-Ac-Xyl$p$ were identified, but we were not able to assign the carbons. One of the 2-O-Ac-Xyl$p$ cross peak (δ_C 62.95, δ_H 3.35) showed a NOESY correlation with the peak of acetyl, reinforcing the assignment. The 3-acetyl-xylopyranose (3-O-Ac-Xyl$p$) was assigned as follows: C1 (δ_C 101.40, δ_H 4.48) and C3 (δ_C 74.62, δ_H 4.95).

All the five carbons of β-1,4-D-xylopyranoside (β-D-Xyl$p$) were assigned. The chemical shifts for the carbon are: C1 (δ_C 101.5, δ_H 4.39), C2 (δ_C 73.59, δ_H 3.35), C3 (δ_C 73.89, δ_H 3.42), C4 (δ_C 75.21, δ_H 3.62), C5 (δ_C 63.06, δ_H 3.25/δ_C 63.06, δ_H 3.96) (Figure 4). The six carbons from β-1,4-D-glucopyranoside [(1–4)-β-Glc$p$] were also assigned with the following chemical shifts: C1 (δ_C 102.72, δ_H 4.45), C2 (δ_C 72.72, δ_H 3.02), C3/5 (δ_C 74.62, δ_H 3.49) and C6 (δ_C 60.19, δ_H 3.90) (Figure 4).

Statistical calculation of 2D-HSQC peaks for characterization of tissue-specificity

We used the peak intensities of the assigned cross peaks, and considered those as 100%, as described before, and analyzed them through a biplot (Figure 5). Considering the biplot data of the samples (Figure 5), seed coat and xylem have higher correlation with C, H, A-S, A-H/G, G, G′, S′, X1 signals and acetylated xylopyranosides (2-O-Ac-Xyl$p$, 3-O-Ac-Xyl$p$, α-D-Xyl$p$, and β-1,4-D-Xyl$p$ polysaccharides signals. In contrast, pith, bark have a higher correlation with H, β-1,4-Glc$p$, α-D-Glc$p$, β-Glc$p$-R, β-1,4-Gal$p$, 2-O-Ac-Man$p$, α-D-Man$p$, and α-L-Ara$f$ signals. But among these three samples, pith shows the highest correlation followed by leaf and bark. Stem has an intermediate pattern and kernel has a very unique one, with a high correlation with A and S, but these two signals can be influenced by the high quantity of protein in this tissue (Figure 5). Finally, in comparing seed coat and xylem, the first has a higher correlation
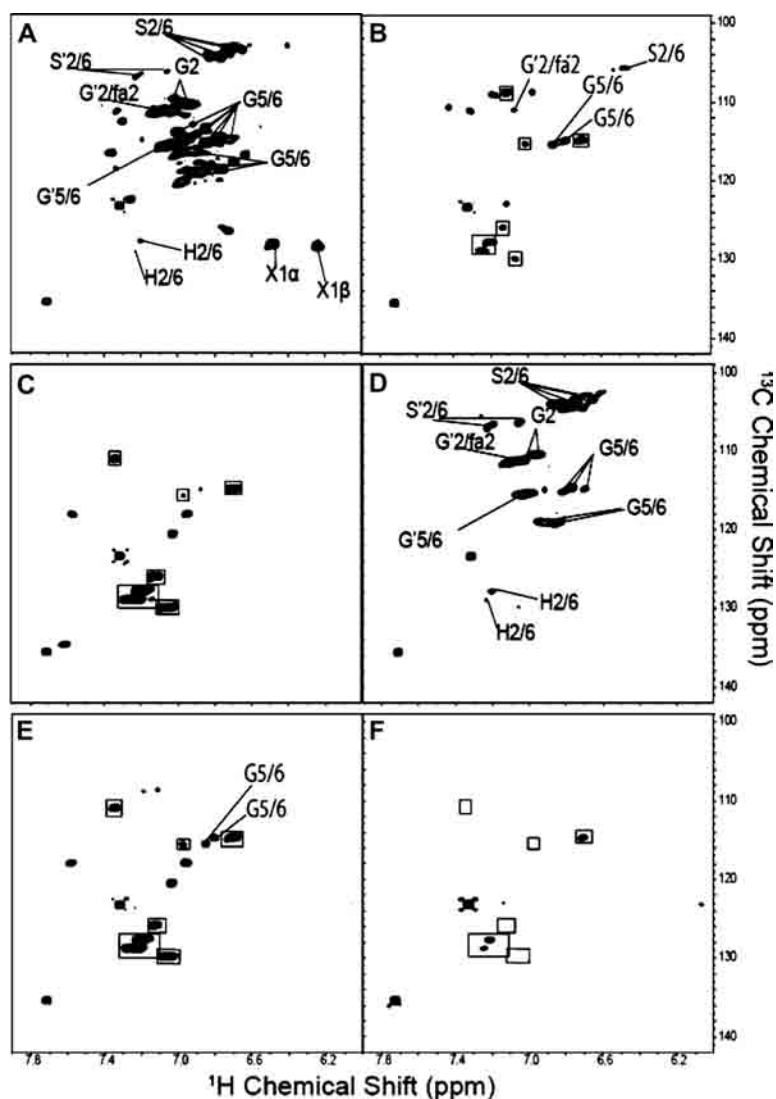
Figure 2.   Aromatic regions of 2D ^{13}C–^{1}H correlation (HSQC) spectra from: a) seed coat; b) bark; c) kernel; d) xylem; e) leaf; f) pith. Syringyl (S), guaiacyl (G), *p*-hydroxyphenyl (H), ferulate (fa) and cinnamyl alcohol (X1). Numbers, *α* and *β* represent the corresponding carbon positions.

Discussion

with C, G′, X1 and B, while the second has a higher correlation with S′, *β*-aryl ether linked to syringyl (A-S), 2-*O*-Ac-Xyl*p*, and *α*-D-Xly*p*. The S/G ratios of these two tissues were 1.989 and 0.242 for xylem and seed coat respectively, showing that xylem is rich in S units and seed coat is rich in G units (Figure 5).

Discussion

The composition of the tissues of xylem and seed coat in NMR HSQC analysis (Figure 5) showed low levels of the *β*-1,4-Glc*p* that can comprise the cellulose of the cell wall. However in FTIR analysis (Figure 1), the peak of hemicellulose and cellulose are of high intensity, especially in the in the case of xylem. The contribution of hemicellulose could be large, but in the cell wall the principal compound is cellulose and the low level of *β*-1,4-Glc*p* could be due to a low dissolution rate of

cellulose in DMSO-d_6/pyridine-d_5 or insufficient ball mill treatment, because of the influence of lignification of these two tissues. NMR data are based on the dissolved part of the samples; therefore, it is important to make an additional comparison of the FTIR data that are obtained for samples in the solid state.

These two tissues present higher correlation with 2-*O*-Ac-Xyl*p*, 3-*O*-Ac-Xyl*p* and *β*-1.4-D-Xyl*p* (Figure 5). The major component of the angiosperm hemicellulose is an *O*-acetyl-4-*O*-methylglucurono-*β*-D-Xylan, found at about 16% in aspen and 13% in kenaf cell wall material (Davis 1998). In *Eucalyptus urograndis* it mainly comprises (1-4)-*β*-D-Xyl*p* (51%), 2-*O*-Ac-Xyl*p* (12%) and 3-*O*-Ac-Xyl*p* (20%) (Magaton and Veloso 2008). Xylem and seed coat have higher correlation with 2-*O*-Ac-Xyl*p* than with 3-*O*-Ac-Xyl*p*, but *O*-acetyl migration during isolation methodologies makes this estimation difficult (Reicher et al. 1984). Therefore xylem and seed coat
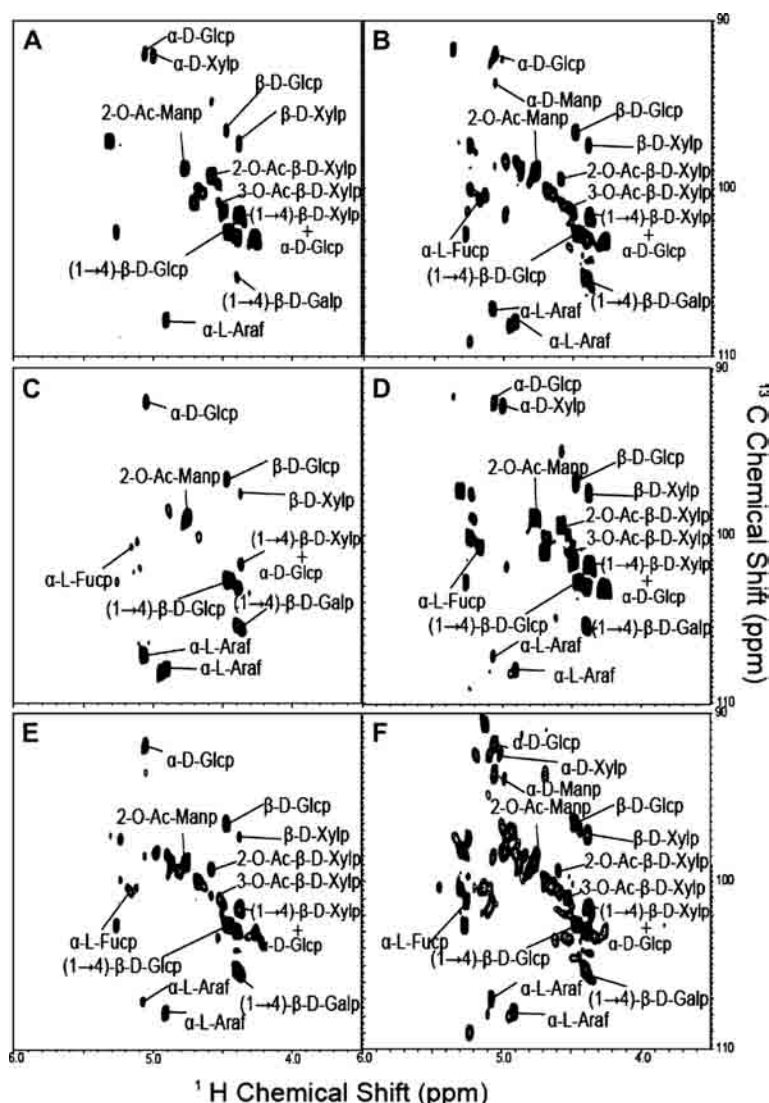
Figure 3. Polysaccharide anomeric regions of 2D ^{13}C–^{1}H correlation (HSQC) spectra from: a) seed coat; b) bark; c) kernel; d) xylem; e) leaf; f) pith; (1–4)-β-D-xylopyranoside [(1–4)-β-D-Xylp], (1–4)-β-D-glucopyranoside [(1–4)-β-Glcp], α-L-fucopyranoside (α-L-Fucp), α-D-glucopyranoside (α-D-Glcp), α-D-xylopyranoside (α-D-Xylp), β-D-glucopyranoside (β-D-Glcp), β-D-xylopyranoside (β-D-Xylp), α-D-mannopyranoside (α-D-Manp), acetylated-β-D-mannopyranoside (2-*O*-Ac-β-D-Manp), acetylated-β-D-xylopyranoside (3-*O*-Ac-β-D-Xylp), acetylated-β-D-xylopyranoside (2-*O*-Ac-β-D-Xylp), (1–4)-β-D-galactopyranoside [(1–4)-β-Galp], α-L-arabinofuranoside (α-L-Araf).

possibly accumulate *O*-acetyl-4-*O*-methylglucurono-β-D-Xylan hemicellulose.

Root sample from *Ricinus communis* (Euphorbiaceae) presented S/G ratios of 0.736, 0.139, and 0.25 in xylem, endoderm and hypodermal cell walls, respectively (Zeier et al. 1999). Jatropha xylem exhibits a ratio of 1.99 and higher intensity in S unit peaks in the NMR spectra than do the others tissues. However in FTIR analysis (Figure 1), it displayed the lowest intensity peak due to C–O of syringyl groups. Seed coat has more intense peaks arising from G units in both FTIR and NMR analysis, and the S/G ratio is 0.242. Another difference between the two tissues is the lower level α-L-Fucp, α-L-Araf in seed coat (Figure 3).

Kernel and leaf showed high intensity peaks in the

FTIR spectra (Figure 1) at approximately 1529 cm^{-1} and 1622 cm^{-1}, related to aromatic rings, with the kernel having the highest absorbance; those peaks can be influenced by the aromatic rings from amino-acids. The kernel of *Jatropha curcas* possesses a high quantity of protein at 22–28% (Devappa et al. 2010), and in 2D-NMR spectra it was also possible to observe high intensity characteristic amino-acids cross peaks in the aromatic region (Figure 2) and aliphatic region (data not shown). The kernel shows a low correlation with lignin and polysaccharides (hemicellulose and cellulose) (Figure 5). The FTIR peak of the cellulose and hemicellulose stretch (ca. 1028 cm^{-1}) in this tissue is least intense and the NMR data showed a low level of most of the polysaccharides, especially acetylated

Figure 4.   Anomeric and aliphatic region of 2D HSQC-NOESY in seed coat, the full lines represent the correlation present in TOCSY and NOESY analysis, the dotted lines represent the ones present only in NOESY. 2-acetyl-xylopyranoside (2-*O*-Ac-Xyl*p*), (1–4)-*β*-D-xylopyranoside [(1–4)-*β*-D-Xyl*p*], (1–4)-*β*-D-glucopyranoside [(1–4)-*β*-Glc*p*] and 3-acetyl-xylopyranoside (3-*O*-Ac-Xyl*p*) unknown peaks were assigned. Numbers or *α* following the name of compounds represent the carbons position. Assignment according to past reports of *β*-aryl ether (A), *β*-aryl ether liked to guaiacyl or *p*-hydroxyphenyl (A-H/G), *β*-aryl ether liked to syringyl (A-S), resimol (C), cinnamyl alcohol (X1), methoxyl, acetyl, *α*-D-glucopyranoside (*α*-D-Glc*p*), *α*-D-xylopyranoside (*α*-D-Xyl*p*), *β*-D-glucopyranoside (*β*-D-Glc*p*), *β*-D-xylopyranoside (*β*-D-Xyl*p*), acetylated-*β*-D-mannopyranoside (2-*O*-Ac-*β*-D-Man*p*), (1–4)-*β*-D-galactopyranoside [(1–4)-*β*-Gal*p*] and *α*-L-arabinofuranoside (*α*-L-Ara*f*) were also made.

Figure 5.   Analysis of biplot for the PCA using the intensities of the peaks of the 2D NMR HSQC spectra. The compounds are presented by vectors in red and tissue in black. Schematic representations of each tissue are also presented in the bottom part of the diagram.

xylopiranosides, and lignin (Figure 5). However, high correlation was observed in S and A peaks, but those peaks can be influenced by the amino acids peaks, which can overlap lignin signals in the NMR spectra. Therefore, the kernel possibly has a low level of lignocellulose and a high content of proteins compared with the situation found with the other tissues.

Pith, leaf and bark showed high correlation with

polysaccharides, such as β-1,4-Glc*p*, α-D-Glc*p*, β-Glc*p*-R, β-1,4-Gal*p*, 2-*O*-Ac-Man*p*, α-D-Man*p*, and α-L-Ara*f*, especially in the case of pith, for which the correlation is the highest (Figure 5). They showed a high intensity in S unit peaks in FTIR analysis, but in the NMR analysis these cross peaks exhibit a low correlation. In this case, the C–O syringyl (ca. 1315 cm^{-1}) peak can be influenced by the CH$_2$ wagging band of the cellulose at ca. 1318 cm^{-1}, since they showed a high correlation with β-1,4-Glc*p* on the biplot of the NMR data (Figures 1, 5). Leaf and bark showed lower levels of correlation with the polysaccharides listed above, compared with pith. This may be due to the presence of lignin in those samples confirmed in HSQC analysis in the aromatic regions (Figure 2). In the leaf sample, the vascular tissue, xylem and phloem was included; in this research, bark and phloem were considered one sample and called bark. Xylem has a high correlation with lignin units. Phloem, as reported in past studies, has sclerenchyma cells, which exhibit a high lignification. Therefore, lignin was expected to be found in leaf and bark samples (Love et al. 1998; Ha et al. 1996).

In this study, we noticed that seed coat and xylem accumulate lignin and hemicellulose *O*-acetyl-4-*O*-methylglucurono-β-D-xylan. The lignin composition differs; in xylem the lignin polymer is rich in S units while the seed coat is rich in G units. Pith, leaf and bark accumulate polysaccharides as cellulose and there is an absence of *O*-acetyl-4-*O*-methylglucurono-β-D-xylan hemicellulose, especially in the case of pith. The kernel has a unique pattern, with a low quantity of lignocellulose, but is rich in protein.

Acknowledgments

References

Balaskshin M, Capanema E, Gracz H, Chang H, Jameel H (2010) Quantification of lignin-carbohydrate linkages with high-resolution NMR spectroscopy. *Planta* 233: 1097–1110

Boerjan W, Ralph J, Baucher M (2003) Lignin biosynthesis. *Annu Rev Plant Biol* 54: 519–546

Chen WH, Kuo PC (2011) Torrefaction and co-torrefaction characterization of hemicellulose, cellulose and lignin as well as torrefaction of some basic constituents in biomass. *Energy* 36: 803–811

Chikayama E, Suto M, Nishihara T, Shinozaki K, Kikuchi J (2008) Systematic NMR analysis of stable isotope labeled metabolite mixtures in plant and animal systems: coarse grained views of metabolic pathways. *PLoS ONE* 3: e3805

Chikayama E, Sekiyama Y, Okamoto M, Nakanishi Y, Tsuboi Y, Akiyama K, Saito K, Shinozaki K, Kikuchi J (2010) Statistical indices for simultaneous large-scale metabolite detections for a single NMR spectrum. *Anal Chem* 82: 1653–1658

Davis MW (1998) A rapid modified method for compositional carbohydrate analysis of lignocellulose by high pH anion-exchange chromatography with pulsed amperometric detection (HPAEC/PAD). *J Wood Chem Technol* 18: 235–252

Devappa RK, Makkar HPS, Becker KL (2010) Nutritional, biochemical, and pharmaceutical potential of proteins and peptides from jatropha: review. *J Agric Food Chem* 58: 6543–6555, Review

Fukuda S, Nakanishi Y, Chikayama E, Ohno H, Hino T, Kikuchi J (2009) Evaluation and characterization of bacterial metabolic dynamics with a novel profiling technique, real-time metabolotyping. *PLoS ONE* 4: e4893

Gilbert HJ (2010) The biochemistry and structural biology of plant cell wall deconstruction. *Plant Physiol* 153: 444–455

Ha MA, Evans BW, Jarvis MC, Apperley DC, Kenwright AM (1996) CP-MAS NMR of highly mobile hydrated biopolymers: polysaccharides of Allium cell walls. *Carbohydr Res* 288: 15–23

Ibarra D, Chávez MI, Rencoret J, Del Río JC, Gutiérrez A, Romero J, Camarero S, Martínez MJ, Jiménez-Barbero J, Martínez AT (2007) Lignin modification during Eucalyptus globulus kraft pulping followed by totally chlorine-free bleaching: a two-dimensional nuclear magnetic resonance, Fourier transform infrared, and pyrolysis-gas chromatography/mass spectrometry study. *J Agric Food Chem* 55: 3477–3490

Ke J, Laskar DD, Chen S (2011) Biodegradation of hardwood lignocellulosics by the western poplar clearwing borer, *Paranthrene robiniae* (Hy. Edwards). *Biomacromolecules* 12: 1610–1620

Kikuchi J, Shinozaki K, Hirayama T (2004) Stable isotope labeling of Arabidopsis thaliana for an NMR-based metabolomics approach. *Plant Cell Physiol* 45: 1099–1104

Kikuchi J, Hirayama T (2007) Practical aspects of stable isotope labeling of higher plants for a hetero-nuclear multi-dimensional NMR-based metabolomics. *Methods Mol Biol* 358: 273–286

Kikuchi J, Ogata Y, Shinozaki K (2011) ECOMICS: ECosytem trans-OMICS tools and methods for complex environmental samples and datasets. *J Ecosys Ecogr* S2: e001

Kim H, Ralph J (2010) Solution-state 2D NMR of ball-milled plant cell wall gels in DMSO-*d*$_6$/pyridine-*d*$_5$. *Org Biomol Chem* 8: 576–591

Kubo S, Kadla JF (2005) Hydrogen bonding in lignin: a Fourier transform infrared model compound study. *Biomacromolecules* 6: 2815–2821

Kumar A, Sharma S (2008) An evaluation of multipurpose oil seed crop for industrial uses (*Jatropha curcas* L.): A review. *Ind Crops Prod* 28: 1–10

Love GD, Snape CE, Jarvis MC (1998) Comparison of leaf and stem cell-wall components in barley straw by solid-state ^{13}C NMR. *Phytochemistry* 49: 1191–1194

Magaton AS, Veloso DP, Colodette JL (2008) Caracterização Das *O*-Acetil-(4-*O*-Metilglicurono) Xilanas Isoladas Da Madeira De *Eucalyptus urograndis*. *Quim Nova* 31: 1085–1088

Manurung R, Wever DAZ, Wildschut J, Venderbosch RH, Hidayat H, Dam JEG, Leijenhorst EJ, Broekhuis AA, Heeres HJ (2009) Valorization of *Jatropha curcas* L. Plant parts: Nut shell

conversion to fast pyrolysis oil. *Food Bioprod Process* 87: 187–196

Mochida K, Furuta T, Ebana K, Shinozaki K, Kikuchi J (2009) Correlation exploration of metabolic and genomic diversities in rice. *BMC Genomics* 10: e563

Nakanishi Y, Fukuda S, Chikayama E, Kimura Y, Ohno H, Kikuchi J (2011) Dynamic omics approach identifies nutrition-mediated microbial interactions. *J Proteome Res* 10: 824–836

Ogata Y, Chikayama E, Morioka Y, Everroad RC, Shino A, Matsushima A, Haruna H, Moriya S, Toyoda T, Kikuchi J (2012) ECOMICS: a web-based toolkit for investigating the biomolecular web in ecosystems using a trans-omics approach. *PLoS ONE* 7: e30263

Okamoto M, Tsuboi Y, Chikayama E, Kikuchi J, Hirayama T (2009) Metabolomic movement upon abscisic acid and salicylic acid combined treatments. *Plant Biotechnol* 26: 551–560

Openshaw K (2000) A review of *Jatropha curcas*: an oil plant of unfulfilled promise. *Biomass Bioenergy* 19: 1–15

Pandey KK (1999) A study of chemical structure of soft and hardwood and wood polymers by FT-IR spectroscopy. *J Applied Sci* 71: 1969–1975

Ralph J, Akiyama T, Kim H, Lu F, Schatz PF, Marita JM, Ralph SA, Reddy MSS, Chen F, Dixon RA (2006) Effects of coumarate 3-hydroxylase down-regulation on lignin structure. *J Biol Chem* 281: 8843–8853

Reicher F, Correa JBC, Gorin PAJ (1984) Location of *O*-acetyl groups in the acidic D-xylan of *mimosa scabrella* (*bracatinga*). A study of *O*-acetyl group migration. *Carbohydr Res* 135: 129–140

Sekiyama Y, Chikayama E, Kikuchi J (2010) Profiling polar and semi-polar plant metabolites throughout extraction processes using a combined solution-state and HR-MAS NMR approach. *Anal Chem* 82: 1643–1652

Tian CJ, Chikayama E, Tsuboi Y, Kuromori T, Shinozaki K, Kikuchi J, Hirayama T (2007) Top-down phenomics of *Arabidopsis thaliana*—One and two-dimensional NMR metabolic profiling and transcriptome analysis of albino mutants. *J Biol Chem* 282: 18532–18541

Yelle DJ, Ralph J, Frihart CR (2008) Characterization of nonderivatized plant cell walls using high-resolution solution-state NMR spectroscopy. *Magn Reson Chem* 46: 508–517

Zeier J, Goll A, Yokoyama M, Karahara I, Schreiber L (1999) Structure and chemical composition of endodermal and rhizodermal/hypodermal walls of several species. *Plant Cell Environ* 22: 271–279